Raman Study of Metallic Tungsten Bronzes

J. F. Scott and R. F. Leheny
Bell Telephone Laboratories, Holmdel, New Jersey 07733
and
J. P. Remeika
Bell Telephone Laboratories, Murray Hill, New Jersey 07974
and
A. R. Sweedler*†
Institute for Pure and Applied Physical Sciences, University of California, San Diego, La Jolla, California
(Received 12 March 1970; revised manuscript received 8 June 1970)

Raman spectra of several metallic tungsten bronzes have been obtained. Cubic $Na_{0.61}WO_3$ exhibits three weak features in the 200–400-cm^{-1} region which are correlated with WO_3 spectra; hexagonal $Rb_{0.30}WO_3$ displays a single broad feature at 655 cm^{-1}; tetragonal $Na_{0.28}WO_3$ has a rich spectrum of 11 features. The presence of a low-energy plasma edge in the bronzes, especially of $Na_{0.28}WO_3$, is responsible for the strong signals obtained; in most metals the reflectivity limits its Raman scattering to a tiny surface layer for laser frequencies below the uv plasma edge. The plasma frequencies for samples used in the present work are determined by reflectivity measurements on single crystals.

I. INTRODUCTION AND EXPERIMENTAL

The tungsten bronzes are a class of high temperature superconductors[1] of general formula M_xWO_3, where M is an alkali metal and $x < 1$. The most extensively studied member of this group is Na_xWO_3, which exhibits metallic behavior for $x \geq 0.2$ and displays several different crystallographic phases. Recently, Dickens and Whittingham have published a review[2] on the general characteristics of tungsten bronzes and their isomorphs.

While many anomalous characteristics of tungsten bronzes have been analyzed experimentally thus far (extremely anisotropic electrical conductivity,[3] high superconducting temperatures which vary radically with alkali concentration,[4] thermal expansion discontinuities,[5] and twinning,[6] etc.), the only optical studies reported have been reflectivity measurements on pellets.[7] Hall measurements[8] demonstrated that each sodium ion in Na_xWO_3 contributes approximately one free electron; the optical data are compatible with that idea and show that the plasma edge shifts in a monotonic way with alkali ion concentration. In the present work, reflectivity measurements on single crystals having $0.28 \leq x \leq 0.61$ have been made and establish the plasma edge as ~5000-7000 Å for such concentrations. This variation results in strikingly different appearances for the samples; all are brightly colored metallic crystals, but they vary in color from deep blue to orange. While this color change is aesthetically interesting, it is also physically important. Most Raman measurements on metals yield very small cross sections owing to the high reflectivity and low penetration depth of visible light. This is due to the presence of the plasma edge in the uv. If one were able to use incident laser light at frequencies above the plasma edge, cross sections would be much larger. In $Na_{0.28}WO_3$, $Rb_{0.3}WO_3$, and $Na_{0.6}WO_3$ we are able to do just that.

The experimental Na_xWO_3 samples used in the present work were grown by electrolysis of a fused melt of tungsten trioxide and sodium carbonate in an argon atmosphere at ~ 800 °C. The $x = 0.61$ samples were orange masses of interpenetrating cubes, each cubic crystallite having mean dimension of about 2 mm. The $x = 0.28$ samples were aggregates of thin blue needles, individually ~ $0.1 \times 0.1 \times 3$ mm. The $Rb_{0.30}WO_3$ samples were hexagonal, ~ 1 mm per side, and prepared as the sodium bronzes with the replacement of Na_2WO_4 by Rb_2WO_4 in the melt. The samples were cleaned in boiling water to remove residual WO_3 and Na_2WO_4 (or Rb_2WO_4) prior to recording of the Raman spectra.

Spectra of each sample were obtained with a backscattering geometry with ~ 400 mW of either 4880-Å or 5145-Å argon ion excitation; the beam was focused onto a single crystal face in each case. Each sample was studied with each laser excitation frequency in order to insure that the observed features were not luminescence. Detection was by means of a Spex 1400 double monochromator, a cooled EMI-6256 photomultiplier, and a Keithley 610B electrometer.

Typcial spectra from a cubic $Na_{0.61}WO_3$ sample are shown in Fig. 1, where comparison is made with pure WO_3. This comparison is useful, despite several phase transitions in WO_3, in that the strong features shown at about 290 and 340 cm^{-1} persist through four of the phases, and hence may

be regarded as typical of the WO_3 distorted perovskite lattice. The $Na_{0.61}WO_3$ spectra shown are weak; they were recorded with 18-sec time constants and 300-μm slit widths.

By comparison, the $Na_{0.28}WO_3$ spectra shown in Fig. 2 are extremely strong. We believe that this strength is due primarily to the tetragonal structure, as discussed in Sec. II, since the plasma frequency in both cubic and tetragonal samples was below that of the laser used. Some resonant enhancement may also be operative in the tetragonal samples, since the deep blue color of these samples is nearly the same as that of the 4880-Å laser; the stronger scattering with 4880-Å excitation compared to that at 5145 Å is compatible with that idea.

Figure 3 illustrates the reflectivity spectrum of two samples: tetragonal $Na_{0.28}WO_3$ and cubic $Na_{0.6}WO_3$ crystals. This figure shows the reflectivity over a region of the visible spectra extending through the reflection minimum resulting when the dielectric contribution of the free carriers just cancels that of the lattice. These results were obtained using standard reflection measurement apparatus comprised of a $\frac{1}{2}$-m Bausch and Lomb spectrometer with tungsten lamp as a source, and a EG&G silicon detector. Wavelength resolution is approximately 16 Å. Aluminum coated spherical mirrors were used to focus the light onto the sample and to collect the reflected light. In addition, a flat aluminum coated mirror was placed in the sample position to provide a reference signal. No attempt has been made to correct for the variation in the reflectivity of the aluminum over the wavelength range used, but the variation is expected to be small.

We have taken the reflectivity at the longest wavelength measured (λ_{max}) equal to unity, and the remaining points are referred to the reflectivity at that wavelength. Absolute reflectivity at any wavelength would be difficult to determine, especially for the samples used, since it requires

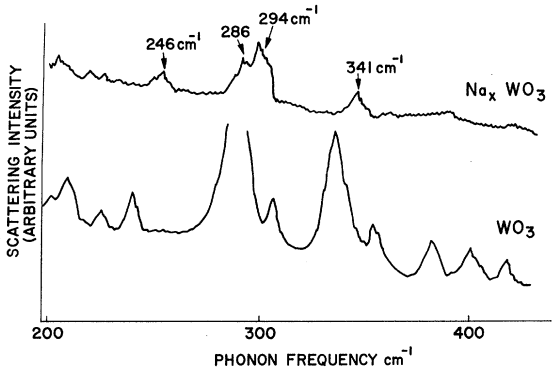

FIG. 1. Raman spectra of $Na_{0.61}WO_3$ and pure WO_3 at 300 °K (unpolarized).

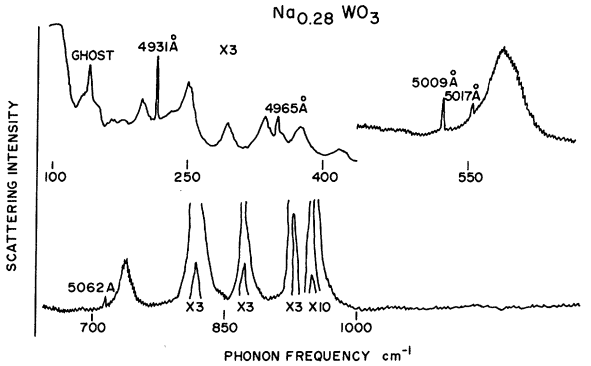

FIG. 2. Raman spectrum of $Na_{0.28}WO_3$ at 300 °K, using 4880-Å excitation. The spectrum shown is unpolarized. No polarization discrimination was possible for scattering from the polycrystalline sample. An identical spectrum was obtained with 5145-Å excitation. Argon emission lines have wavelengths marked over them.

knowledge of the area of the sample scattering light into the collection optics, as well as the incident light intensity.

For the purpose of evaluating the data we have computed a theoretical reflection spectra for a sample assumed to have a short-wavelength refractive index K = 3.4, and a free-electron collision frequency $\nu = \frac{1}{20}\omega_p$, where ω_p is the free-electron plasma frequency $\omega_p = e^2n/mK^2$. These values provide reasonable agreement to the trends in the data. The theoretical curve is generated using

$$R = [(\mu - 1)^2 + \chi^2] / [(\mu + 1)^2 + \chi^2] ,$$

with μ and χ related in the usual way to the lattice index and with the free-carrier contribution calcu-

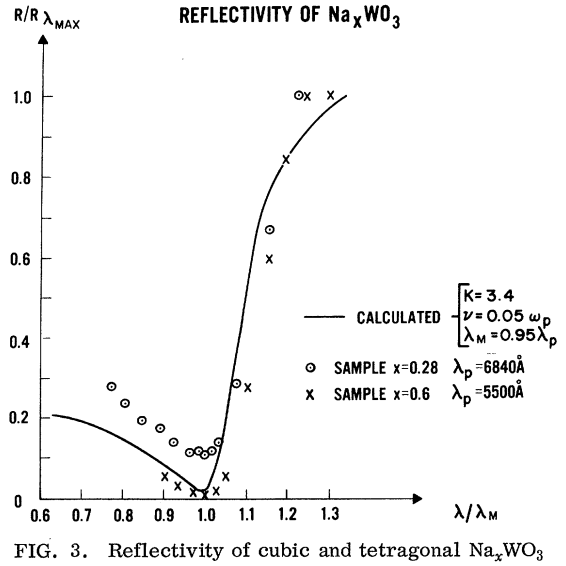

FIG. 3. Reflectivity of cubic and tetragonal Na_xWO_3 single crystals, illustrating well-defined dips at the plasma frequency.

lated using the Drude theory. For the lattice index chosen we find that the reflection minimum λ_m, occurs when $\lambda/\lambda_p = 0.95$, where now λ_p is the vacuum wavelength corresponding to the free-carrier plasma frequency. Since both μ and χ can be expressed in terms of normalized frequency λ/λ_p, and the dimensionless constant ν/ω_p, a single curve can describe the reflectivity for all crystals having the same short-wavelength index and relative electron collision frequency.

There are a number of factors which influence the accuracy of these results. First, we have neglected any dispersion in the lattice contribution to the index over the range of our measurements; this dispersion would contribute additional wavelength variation of the reflectivity. In addition, we have taken the same value of short-wavelength index for both samples although it might well vary with the concentration of sodium. Finally, since the measurements were not continued very far into the infrared, there is the possibility that the peak reflectivity might be as much as 10—15% higher than that measured at the longest wavelength shown. Such a possibility would not effect the wavelength for minimum reflection measurement, but would tend to reduce the indicated short-wavelength reflection, thereby reducing the calculated index and make λ_p more nearly equal to λ_m. Since we have used a value of $\lambda_m = 0.95\ \lambda_p$, the maximum error, due to overestimation of K, in determining λ_p is only 5%.

Although we would naively expect the Raman scattering to be greatest for $\omega_{\text{laser}} \approx \omega_p$, as determined from the influence of reflectivity $R(\omega)$ on penetration depth, we have experimentally found Raman intensity to be greater (with laser wavelength at 4880 Å) in samples with $\lambda_p = 6840$ Å than in those with $\lambda_p = 5500$ Å. This difference may relate to free-carrier absorption, resonant enhancement factors not related to plasma effects, and other structural parameters discussed below, since the samples having different plasma frequencies also had different lattice structure. It seems likely from a qualitative standpoint that the much greater Raman cross sections in $Na_{0.28}WO_3$ and $Rb_{0.3}WO_3$ compared with those in $Na_{0.6}WO_3$ can be attributed primarily to the differing crystal structures, rather than to the different plasma frequencies with the plasma playing only a small role for laser wavelength $\lambda > \lambda_p$. Further studies in the future on cubic $Na_{0.4}WO_3$ will help confirm that judgement.

II. PHONON ANALYSIS AND DISCUSSION

Previous Raman studies of metals[9] have been restricted to simple diatomic lattices in which there was no need for complex analysis of the spectra. By comparison, the $Na_{0.28}WO_3$ spectrum summarized in Table I and Fig. 2 is quite complex.

The strong scattering in the region 700—1000 cm^{-1} is analogous to that observed in other crystals with tungsten-oxygen bonds. Pure WO_3 has its W-O stretching modes at 717 and 808 cm^{-1}.[10] The higher frequencies in Na_xWO_3 (813 and 928 cm^{-1} for the strong modes) are compatible with a simple physical picture in which the filling of empty Na sites makes the lattice more rigid. We note that phonons in insulating tungstates of form MWO_4 usually have greatest Raman cross sections[11] in the 700—1000-cm^{-1} region, like WO_3. In this respect, high-frequency W-O stretching modes are rather independent of the specific bonding arrangement in the lattice. Their strong Raman spectra reflects the fact that oxygen ions are extremely polarizable.

The low-frequency spectra (< 400 cm^{-1}) in Na_xWO_3 are almost impossible to assign in terms of simple models and symmetry coordinates in these nonstoichiometric compounds.

It is possible to make some comments regarding the broad mode at 592 cm^{-1} in $Na_{0.28}WO_3$. In other perovskites, such as $SrTiO_3$ and $KTaO_3$, the highest-frequency transverse optical phonon also lies in the 550-cm^{-1} region. This is a frequency region from which modes are conspicuously absent in $M^{2+}WO_4$ lattices,[11] and hence it appears to be associated with the perovskite structure *per se*. To some extent, therefore, it may be describable in terms of Cowley's shell-model-determined eigenvectors.[12] The large linewidth of this mode is not understood at present. It may be that the deviation from stoichiometric distribution of Na ions in the lattice contributes to the linewidth of some modes more than others (we recall that glasses such as silica and germania usually exhibit both broad and narrow Raman features); however, there is nothing in Cowley's model[12] which leads us to believe that the highest TO in the ABO_3 perovskite lattice

TABLE I. Optical-mode frequencies in $Na_{0.28}WO_3$ (cm^{-1}). (vs, s, m, w characterize scattering intensities as very strong, strong, medium, or weak.)

$Na_{0.28}WO_3$
961 (vs)
936 (s)
880 (s)
831 (vs)
757 (m)
592 (s, broad)
421 (w)
373 (w)
333 (w)
294 (w)
248 (w)

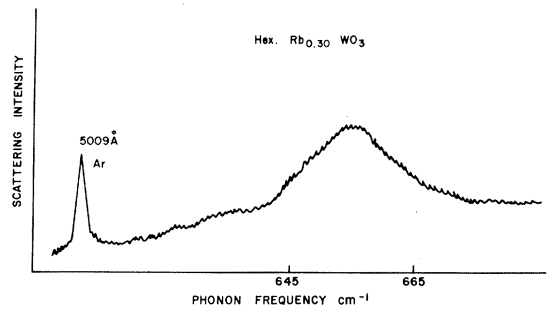

FIG. 4. Polarized α_{xx} (x in plane of surface) spectrum of $Rb_{0.30}WO_3$ at 300 °K.

should involve the A atoms in any special way. An alternative approach to the linewidth of this mode is to consider the model[13] of Mills *et al.* for odd-parity mode scattering in metals. This model predicts a linewidth which is large for very dispersive modes, which could be the case for $Na_{0.28}WO_3$; however, the line shape for such scattering is predicted to be very asymmetric, [13] which is clearly not the case in Fig. 2.

The anomalous mode at 592 cm^{-1} in $Na_{0.28}WO_3$ becomes especially interesting when we view the spectrum of hexagonal $Rb_{0.3}WO_3$ in Fig. 4. This spectrum consists of a single feature which is broad and centered at 655 cm^{-1}. We interpret this mode as the analog of the 592-cm^{-1} feature in $Na_{0.28}WO_3$. We cannot explain the absence of other sharper features in the spectrum. The only explanation we can suggest is qualitative. In the undistorted, cubic perovskite lattice, there is no first-order Raman spectrum. The weak scattering in cubic $Na_{0.6}WO_3$ arises from the relaxed translational symmetry due to sodium vacancies. In contrast, the strong scattering in tetragonal $Na_{0.28}WO_3$ arises primarily from the tetragonal lattice distortion, which greatly increases the size of the unit cell and the number of Raman modes, even assuming perfect stoichiometry.[1] (This helps explain the modes in the 700—1000-cm^{-1} region which are absent in the $Na_{0.6}WO_3$ cubic sample.) The hexagonal $Rb_{0.3}WO_3$ unit cell ($z = 6$) is substantially smaller than the tetragonal, which partially explains the absence of Raman features. It is also possible that the sharp lines in the $Na_{0.28}WO_3$ spectra arise from nonmetallic Na_xWO_3 ($x < 0.2$) regions at the surface. Further studies on samples with different surface treatments (polish, etch) should clarify the origin of these sharp lines.

III. SUMMARY

In summary, we have presented Raman data on the only complex metals examined thus far. We have attributed strong scattering to the measured presence of the plasma edge at wavelengths longer than that of the laser used as excitation source. We qualitatively interpret the large number of modes in $Na_{0.28}WO_3$ as due to the much larger unit cell in the tetragonal bronzes, as compared to cubic Na_xWO_3 or hexagonal $Rb_{0.3}WO_3$. We observe anomalously broad features at ~600 cm^{-1} in both tetragonal and hexagonal bronzes.

While this work is admittedly preliminary, it does represent the only Raman study of complex metals, and we hope it will stimulate other experimental and theoretical investigations.

Since members of this class of crystals superconduct as high[4] as 6.5 °K, the obvious extension of the present study is Raman scattering near and below T_c.

Note added in manuscript. After this work was submitted, G. H. Taylor[14] reported reflectivity data for samples of Na_xWO_3 with $x \approx 0.6$ in agreement with our results.

ACKNOWLEDGMENTS

We would like to thank L. E. Cheesman for excellent technical assistance and Professor B. T. Matthias and Dr. J. P. Gordon for their encouragement of this work. We also would like to thank Dr. J. L. Shay for generously making available his laboratory facilities for the measurements of the reflectivity spectra.

*Present address: Departmento de Fisica, Facultad de Ciencias, University de Chile, Santiago, Chile.

†Research at the University of California sponsored by the Air Force Office of Scientific Research, under Grant No. AF-AFOSR 631-67.

[1]A complete review emphasizing superconducting properties may be found in A. R. Sweedler, Ph. D. thesis, University of California, San Diego, 1969 (unpublished).

[2]P. G. Dickens and M. S. Whittingham, Quart. Rev. (London) 22, 30 (1968).

[3]L. D. Muhlestein and G. C. Danielson, Phys. Rev. 158, 825 (1967).

[4]Ch. J. Raub, A. R. Sweedler, M. A. Jensen, S. Broadston, and B. T. Matthias, Phys. Rev. Letters 13, 746 (1964); A. R. Sweedler *et al.*, *ibid.* 15, 108 (1965); J. P. Remeika *et al.*, Phys. Letters 24A, 565 (1967).

[5]C. Rosen, B. Post, and E. Banks, Acta Cryst. 9, 477 (1956); Takeshi Takamori and Minoru Tomozawa, J. Am. Ceram. Soc. 47, 9 (1964).

[6]J. H. Ingold and R. C. DeVries, Acta Met. 6, 736 (1958).

[7]B. W. Brown and E. Banks, J. Am. Chem. Soc. 76, 1963 (1954). The x value for the cubic bronze ($x = 0.61$) was determined by measuring the lattice parameter and calculating x from the Brown and Banks relationship. The x values for the tetragonal Na bronze ($x = 0.28$) and the hexagonal Rb bronze ($x = 0.3$) were estimated by taking x-ray powder patterns and comparing the results with

those of Magneli. In all cases, it was possible to index every line as belonging to the bronze pattern. A. Magneli, Arkiv. Kemi 1, 269 (1949); Acta. Chem. Scand. 7, 315 (1953).

[8]W. R. Gardner and G. C. Danielson, Phys. Rev. 93, 46 (1954); G. C. Danielson, *ibid.* 158, 825 (1967).

[9]D. W. Feldman, J. H. Parker, Jr., and M. Ashkin, Phys. Rev. Letters 21, 607 (1968); in *Light Scattering Spectra of Solids*, edited by G. B. Wright (Springer, New York, 1969).

[10]Preliminary reports of this work were given at APS meetings in 1969 and 1970: J. F. Scott, Bull. Am. Phys. Soc. 14, 738 (1969); 15, 327 (1970).

[11]J. F. Scott, J. Chem. Phys. 49, 98 (1968).

[12]R. A. Cowley, Phys. Rev. 134, A981 (1964).

[13]D. L. Mills, A. A. Maradudin, and E. Brustein, in *Light Scattering Spectra of Solids*, edited by G. B. Wright (Springer, New York, 1969).

[14]G. H. Taylor, J. Solid State Chem. 1, 359 (1970).

PHYSICAL REVIEW B VOLUME 2, NUMBER 10 15 NOVEMBER 1970

Magnetostriction of Paramagnetic Transition Metals. II. Group-VIII Metals Ru, Rh, Pd, Ir, Pt, and Their Alloys

E. Fawcett*
Bell Telephone Laboratories, Murray Hill, New Jersey 07974
(Received 12 June 1970)

The longitudinal magnetostriction of group-VIII transition metals and alloys was measured with a capacitance dilatometer at 4.2 °K in fields up to 100 kOe. The resultant values of the logarithmic volume dependence of the magnetic susceptibility, $\partial \ln\chi/\partial \ln V$, are Ru, −4.8; Rh, 9.6; Pd, −3.4; Ir, 22; Pt, −15; $Rh_{50}Ir_{50}$, 15; $Rh_{50}Pd_{50}$, 8; $Ir_{40}Pd_{40}$, 14; $Pd_{67}Pt_{33}$, −4; and $Pd_{33}Pt_{67}$, −24. Pd, Pt, and their alloys have a negative magnetostriction, which indicates a negative volume dependence of the Coulomb interaction responsible for the exchange enhancement of their spin susceptibility. Rh, Ir, and their alloys with each other and with Pd have a positive magnetostriction, and the resultant large volume dependence of the susceptibility, particularly that of Ir, is difficult to understand. Float-zoned samples of Rh and Ir exhibit oscillatory de Haas–van Alphen magnetostriction at 4.2 °K.

I. INTRODUCTION

In this paper we describe longitudinal magnetostriction measurements on several group-VIII metals and alloys. The experimental procedure was described in a previous paper,[1] where we reported similar measurements on group-IV, -V, and -VI transition metals. The magnetostriction provides a measure of the volume dependence of the magnetic susceptibility, which in Pd and Pt is dominated by the exchange-enhanced Pauli paramagnetism. In these metals and their alloys the magnetostriction is negative, which indicates a negative volume dependence of the Coulomb interaction. In Rh and Ir and their alloys with each other and with Pd, the volume dependence of the susceptibility is large and positive. The very large value for Ir is particularly difficult to understand. Pure samples of Rh and Ir exhibited oscillatory de Haas–van Alphen magnetostriction, which we describe briefly pending a thorough study of the effect in these metals.

II. EXPERIMENTAL

The experimental techniques for measuring the magnetostriction were described in Ref. 1. The samples are described in Table I. Because traces of Fe can affect the low-temperature susceptibility of several of these metals to a marked degree, we give the Fe content when it is available.

The magnetostriction of the group-VIII metals up to 100 kOe at a temperature 4.2 °K is shown in Figs. 1 and 2. The samples Rh*A* and Ir*A* were

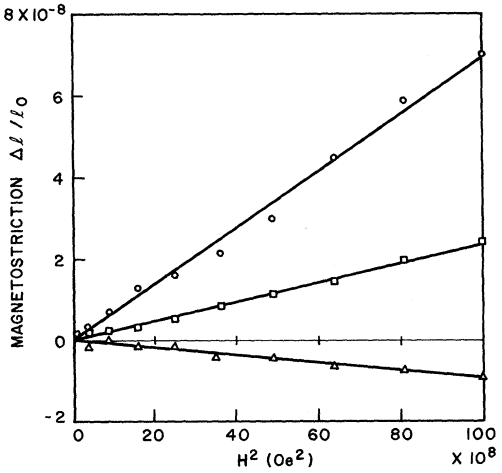

FIG. 1. Magnetostriction of Ru, Rh, and Ir: △, Ru; ○, Rh; □, Ir.